Journal of Associated Medical Sciences 2018; 51(3): 138-149

JAMS
Journal of Associated Medical Sciences

Thai-Journal Citation Index Centre (TCI) & ASEAN Citation Index (ACI)

Journal of Associated Medical Sciences

Journal homepage: https://www.tci-thaijo.org/index.php/bulletinAMS/index

Dosimetric validation of the eclipse Acuros XB dose calculation algorithm for a 6 MV photon beams

Taweap Sanghangthum[1*] Yot Phimmakone[2] Sivalee Suriyapee[1]

[1]Division of Radiation Oncology, Department of Radiology, Faculty of Medicine, Chulalongkorn University, Bangkok, Thailand.
[2]Radiotherapy center, Mittaphab Hospital, Ministry of Health, Vientiane, Laos.

ARTICLE INFO

Article history:
Received 23 May 2018
Accepted as revised 24 June 2018
Available online 4 August 2018

Keywords:
Acuros XB; dose accuracy; IAEA TRS 430; IMRT; VMAT

ABSTRACT

Background: Acuros XB (AXB) is a novel algorithm implemented to the commercial vender of Varian Eclipse treatment planning system. It is developed to improve the accuracy of dose calculation in external beam radiotherapy, especially in heterogeneity region.

Objectives: To evaluate dosimetric impact of AXB algorithm in basic beam characteristics and clinical applications according to IAEA TRS 430 protocol.

Materials and methods: Scanning percentage depth doses (PDDs) from CC13 ionization chamber and beam profiles at 10 cm depth from PFD diode of 6 MV from TrueBEAM linear accelerator were obtained in water phantom. Output factors were measured at 10 cm depth using CC13 chamber. Doses of fifteen cases in each 3D-CRT, IMRT, and VMAT techniques in solid phantom and CIRS thorax phantom were measured with CC13 chamber. All measurement results were compared with calculation from Eclipse treatment planning system (TPS) using AXB algorithm.

Results: The results showed good agreement between measured and calculated PDDs with δ_1 (high dose & small dose gradient) less than 1.5% and δ_2 (high dose & large dose gradient) within 1.5 mm. Measured profiles also displayed the coincidence results with TPS, which showed δ_2 less than 2 mm, δ_3 (high dose & small dose gradient) within 3%, δ_4 (low dose & small dose gradient) within 3%, and $\delta_{50\text{-}90}$ within 2 mm as the recommendation from IAEA TRS 430 protocol. Maximum output factors differences were only -1.54%. Clinical plans exhibited the dose differences between measurement and calculation in 3D-CRT, IMRT, and VMAT of -0.12±0.38%, -1.59±0.93%, and 0.87±1.24% for homogeneous phantom and 0.27±0.29%, -0.60±1.05%, and -1.12±0.44% for inhomogeneous phantom, respectively.

Conclusion: Dose differences between measurement and AXB algorithm calculation are within the recommendation of IAEA TRS 430. AXB algorithm is acceptable for dose calculation in external beam radiotherapy.

Introduction

Radiation therapy is one of the most common methods for cancer treatment by delivering high radiation dose to the tumor while avoiding the normal tissues from doses receiving above the limitations. The accurate dose calculation in clinical situation is important to the modern practice of radiotherapy. New treatment calculation algorithm can increase the capability in accuracy and precision of radiation dose calculation. Acuros XB (AXB) is a novel algorithm implemented to the commercial vender of Varian Eclipse treatment planning system (TPS) (Varian Medical System, Palo Alto, CA) that was developed to administer accuracy and speed in delivering radiation in external beam

* **Corresponding author.**
Author's Address: Division of Radiation Oncology, Department of Radiology, Faculty of Medicine, Chulalongkorn University, Bangkok, Thailand.
** **E-mail address:** mairt34@yahoo.com
doi: 10.14456/jams.2018.19
E-ISSN: 2539-6056

radiotherapy. The linear Boltzmann transport equation is used in this algorithm to mainly improve dose calculation accuracy of heterogeneity materials in patient's body such as lung, bone, air, or non-biologic implants.[1,2,3] This equation is a set of partial differential equations that govern the transport of particles or radiation through matter. The testing of TPS is recommended as a radiotherapy quality assurance framework. Hoffman L et al.[4] and Zlfodya JM el al.[5] evaluated the AXB photon dose calculation algorithm by comparing with previous algorithm, analytical anisotropic algorithm (AAA). They found that output factors and percentage depth doses (PDDs) from AXB were comparable with the data from AAA for the measurement in homogeneous phantom and superior to AAA in heterogeneous phantom. Yeh CY et al.[6] claimed the comparable accuracy of dose distribution to Monte Carlo methods in clinical treatment planning in nasopharyngeal carcinoma.

IAEA Technical Report Series No. 430 (TRS 430) has established the guideline to assist radiotherapy medical physicist to implement the comprehensiveness in commissioning and quality assurance of computerized TPS including software and algorithm for radiation treatment of cancer.[7] This report described the testing methods and defined the acceptability criteria for external beam dose calculation compared with dose measurement.

The purpose of this research was to verify the dosimetric accuracy of AXB algorithm in Eclipse TPS according to IAEA TRS 430 protocol in basic beam characteristics in terms of PDDs, beam profiles, and output factors and in clinical situations in 3D-conformal radiotherapy (3D-CRT), intensity modulated radiotherapy (IMRT) and volumetric modulated arc therapy (VMAT) plans.

Materials and methods

All of the results presented in this research were based on the calculated beam data from Eclipse AXB algorithm version 10.0.31 for a 6 MV photon beams from Varian TrueBeam linear accelerator equipped with a millennium 120 MCL (Varian Medical Systems, Palo Alto, CA, USA).

A. Basic beam characteristics:

The PDDs, in-plane and cross-plane beam profiles and output factors were calculated in virtual water phantom in TPS and compared with the measurement results in Blue phantom (IBA Dosimetry GmbH, Schwarzenbruck, Germany). The PDDs of square field sizes (5x5, 10x10, 20x20, 30x30 cm2) and rectangular field sizes (5x10, 20x10, 30x10 cm^2) were scanned using the CC13 ionization chamber, while the beam profiles at 10 cm depth with the same opening field sizes in PDDs were scanned using PFD diode detector (IBA Dosimetry GmbH, Schwarzenbruck, Germany). The output factors were measured in square field sizes (5x5, 8x8, 12x12, 15x15, 20x20, 25x25, 30x30, 35x35 cm^2) and rectangular field sizes (10x5, 5x10, 5x15, 5x20, 5x30, 10x15, 10x20, 10x25, 10x30, 20x10, 30x10 cm^2) using CC13 chamber in solid water phantom. The PDDs and profiles evaluation was assessed by δ_1, δ_2, δ_3, δ_4 and $\delta_{50\text{-}90}$ parameters according to IAEA TRS 430 [7] and shows in Figure 1. PDD was evaluated in δ_1 (central beam axis for high dose and small dose gradient of the dose difference at 10 cm depth) and δ_2 (build-up region for high dose and large dose gradient of the distance difference at 90% dose), while the profiles were analyzed in δ_2 (beam profile region for high dose and large dose gradient of the distance difference at 40% dose), δ_3 (outside beam central axis for high dose and small dose gradient of the dose difference at 60% of field from central axis), δ_4 (outside beam edges for low dose and small dose gradient of the dose difference at 20% of the field) and $\delta_{50\text{-}90}$ for a beam fringe for the distance difference between 50% and 90% dose).

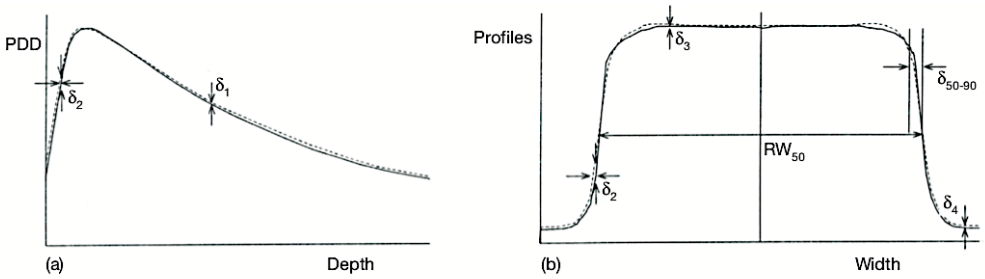

Figure 1 *Regions of dose difference evaluation in (a) percentage depth dose, and (b) profile.*

B. Clinical applications:

This study compared the dose differences between measurement and calculation in clinical applications for three different techniques; those are 2 to 4-field 3D-CRT, 9-field IMRT and 2.5-arc VMAT. The fifteen cases in each technique with all 6 MV beams were randomly selected in head, chest and pelvic regions and calculated with AXB algorithm. All of the clinical plans were recalculated and measured in solid water phantom as the homogeneous medium and in CIRS thorax phantom as the inhomogeneous medium as shown in Figure 2 as the example of VMAT QA plan. The size of solid water phantom is 30x30x30 cm^3 and the isocenter is at center of phantom. The measurements in both phantoms were performed using CC13 ionization

chamber at isocenter position. Even though this study was performed based on the phantoms measurement, the patient plans were selected to recalculate in phantom. The study was reviewed and approved by ethical committees of the Faculty of Medicine, Chulalongkorn University.

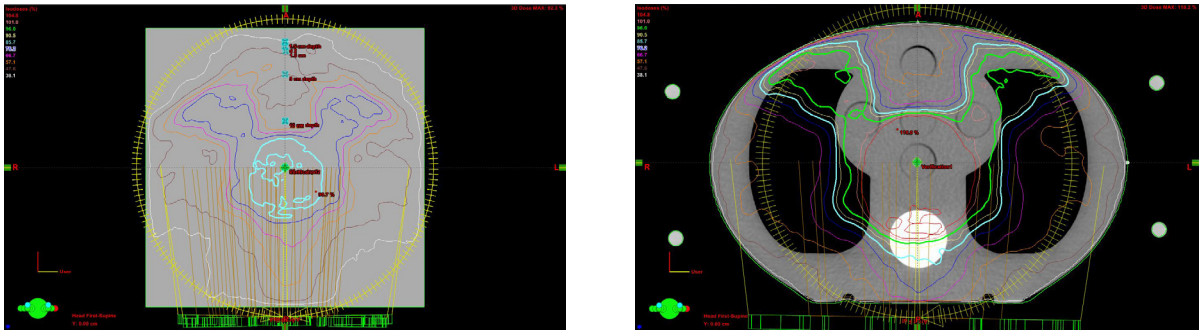

(a) (b)

Figure 2 *VMAT plan at pelvis region recalculated in (a) solid water phantom and (b) CIRS phantom.*

Results

A. Basic beam characteristics:

A.1 Percentage depth doses

Scanning PDD curves along the central axis of 6 MV photon beams in the homogeneous water phantom using CC13 ionization chamber were compared with the calculation from AXB algorithm and presented in some fields in Figure 3. The open square fields are (a) 10x10 cm^2 and (b) 20x20 cm^2, and open rectangular fields are (c) 5x10 cm^2 and (d) 30x10 cm^2. The measured PDD data from CC13 chamber are shown in dotted, while the photon dose from AXB calculations are presented in solid lines.

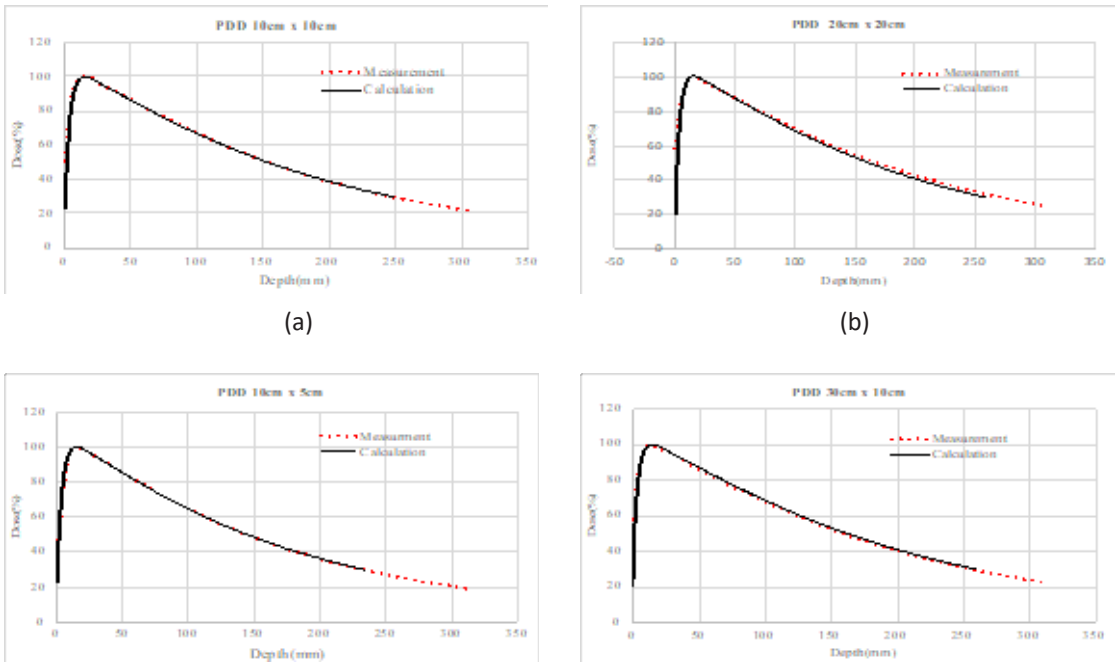

(a) (b)

(c) (d)

Figure 3 *Percentage depth dose curve comparison between measurement and calculation for the square fields of (a) 10x10 cm^2, (b) 20x20 cm^2 and rectangular fields of (c) 5x10 cm^2, (d) 30x10 cm^2.*

Table 1 shows the comparisons of dose differences (δ_1) and distance differences (δ_2) between measurement and calculation for various square and rectangular field sizes. The average dose difference for all test field sizes between measurement and calculation of δ_1 was only 0.16±0.64%, while the average distance difference of δ_2 was 0.43±0.70 mm.

Table 1 Dose (δ_1) and distance (δ_2) differences between measurement and calculation from PDDs in various square and rectangular field sizes for 6 MV photon beams.

Field size (cm^2)	D 10cm depth		δ_1 (%)	d 90% dose		δ_2 (mm)
	Mea. (%)	Cal. (%)		Mea. (mm)	Cal. (mm)	
5x5	62.40	62.97	0.57	6.38	6.98	0.60
10x10	66.47	66.72	0.25	4.59	6.38	0.79
20x20	69.40	68.24	-1.16	5.25	6.36	1.11
30x30	70.90	71.39	0.49	4.65	5.12	0.47
5x10	64.57	64.45	-0.12	7.76	6.68	-1.08
20x10	67.70	68.24	0.54	5.76	6.36	0.60
30x10	68.00	68.58	0.58	5.71	6.25	0.54
Average			**0.16**			**0.43**
Standard deviation			**0.64**			**0.70**

A.2 Beam profiles

Figure 4 displays some beam profiles comparison at 10 cm depth between measurement and calculation for the square fields of (a, e) 10x10 cm^2 and (b, f) 30x30 cm^2 and rectangular field size of (c, g) 5x10 cm^2 and (d, h) 30x10 cm^2 for in-plane and cross-plane, respectively. The measured beam profiles data from CC13 chamber are shown in dotted, while the photon dose from AXB calculations are presented in solid lines. Both in-plane and cross-plane profiles showed very good match between measurement and calculation except the penumbra region and at very low dose.

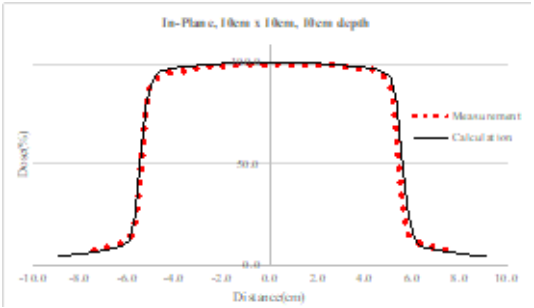

(a)

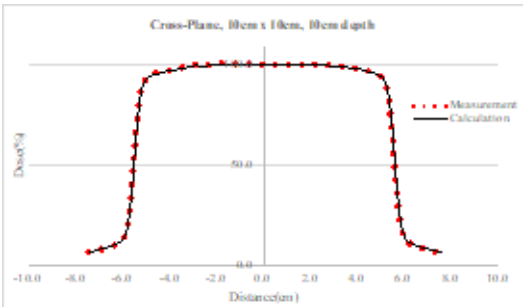

(e)

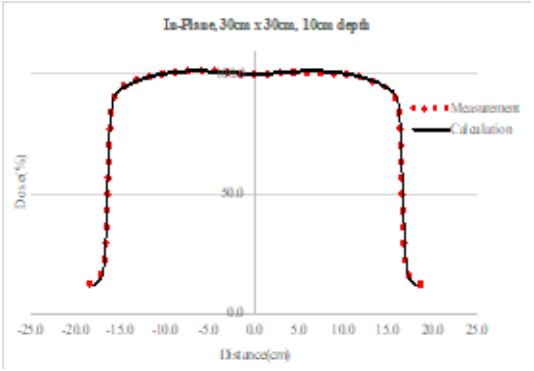

(b)

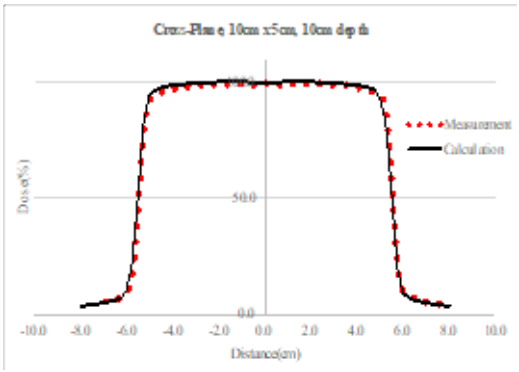

(f)

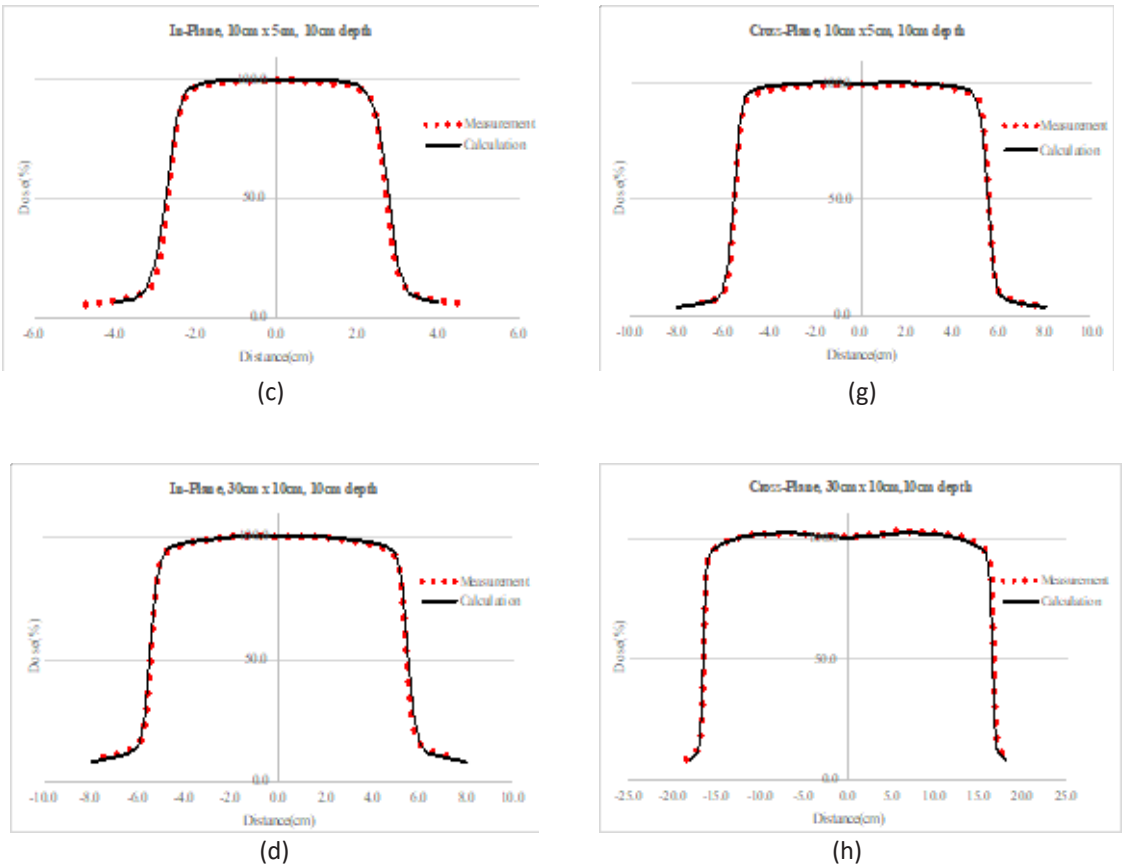

Figure 4 *In-plane (a-d) and cross-plane (e-h) profiles comparison between measurement and calculation for field size of 10x10 cm², 30x30 cm², 5x10 cm², and 30x10 cm², respectively.*

Table 2 In-plane beam profile comparison between measurement and calculation at 10 cm depth in terms of δ_2, δ_3, δ_4 and $\delta_{50\text{-}90}$ for open square and rectangular field sizes.

F.S (cm^2)	In-plane, 10cm depth											
	$d_{40\%\ dose}$ (mm)		δ_2 (mm)	$D_{60\%\ inner\ F.S}$ (%)		δ_3 (%)	$D_{20\%\ outer\ F.S}$ (%)		δ_4 (%)	$d_{50\%\text{-}90\%dose}$ (mm)		$\delta_{50\text{-}90}$ (mm)
	Mea.	Cal.		Mea.	Cal.		Mea.	Cal.		Mea.	Cal.	
5x5	-27.80	-28.34	-1.54	99.22	99.14	-0.08	8.84	7.84	-1.00	3.35	4.53	1.00
10x10	-55.63	-56.20	-0.57	97.45	98.78	1.33	9.12	8.32	-0.80	4.17	4.41	0.24
20x20	-101.06	-111.41	-1.35	100.99	100.02	-0.97	-	-	-	5.41	5.11	-0.30
30x30	-165.25	-166.27	-1.02	100.83	100.51	-0.32	-	-	-	6.95	6.63	-0.33
10x5	-27.85	-28.47	-0.62	98.75	99.21	0.46	11.11	10.20	-0.91	3.54	4.47	0.93
20x10	-55.24	-56.22	-0.98	98.44	98.47	0.03	11.31	10.29	-1.02	4.26	4.58	0.32
30x10	-55.23	-56.27	-1.04	98.25	98.42	0.17	12.14	11.01	-1.13	4.22	4.62	0.40
Average			**-0.87**			**0.09**			**-0.97**			**0.32**
Standard deviation			**0.30**			**0.17**			**0.12**			**0.53**

From Table 2, the average percent dose or distance-to-agreement differences between measurement and calculation of in-plane profile at 10 cm depth for penumbra region of profile for high dose, large dose gradient, δ_2 for 40% dose, was -0.87±0.30 mm with the range from -1.54 mm to -0.57 mm. For the average percent differences of outside central beam axis for high dose and small dose gradient of δ_3 (60% of field size from central axis) was 0.09±0.17% with the range from -0.97% to 1.33%. The average percent difference for outside beam edges for low dose and small dose gradient, δ_4 for 20% of field size from field edge, was -0.97±0.12 % with the range from -1.13% to -0.80%. The average difference for beam fringe for the distance from 50% to 90% was 0.32±0.53 mm with the range from -0.33 mm to 1.00 mm.

Table 3 shows the differences of calculated cross-plane beam profiles from measured data that presents the same trend with the results from Table 2. The average percent deviation between measurement and calculation of cross-plane profile at 10 cm depth for penumbra region of profile for high dose, large dose gradient, δ_2 for 40% dose, was -0.42±0.22 mm with the range from -0.76 mm to -0.09 mm. For the average percent difference of outside central beam axis for high dose and small dose gradient of δ_3 (60% of field size from central axis) was 0.42±0.29% with the range from -0.20% to 0.65%. The average percent difference for outside beam edges for low dose and small dose gradient, δ_4 for 20% of field size from field edge, was -0.73±0.82 with the range from -1.14% to 0.18%. The average difference for beam fringe for the distance from 50% to 90% was 1.02±0.23 mm with the range from 0.53 mm to 1.18 mm.

Table 3 Cross-plane beam profile comparison between measurement and calculation at 10 cm depth in terms of δ_2, δ_3, δ_4 and $\delta_{50\text{-}90}$ for open square and rectangular field sizes.

F.S. (cm^2)	Cross-plane, 10cm depth											
	$d_{40\% \text{ dose}}$ (mm)		δ_2 (mm)	$D_{60\% \text{ inner F.S}}$ (%)		δ_3 (%)	$D_{20\% \text{ outer F.S}}$ (%)		δ_4 (%)	$d_{50\%\text{-}90\%\text{dose}}$ (mm)		$\delta_{50\text{-}90}$ (mm)
	Mea.	Cal.		Mea.	Cal.		Mea.	Cal.		Mea.	Cal.	
5x5	-28.26	-29.02	-0.76	98.73	99.17	0.44	8.07	8.25	0.18	3.25	3.78	0.53
10x10	-56.28	-56.37	-0.09	98.93	98.73	-0.20	9.40	7.99	-1.14	3.93	5.01	1.08
20x20	-111.11	-111.59	-0.48	99.43	100.02	0.59	-	-	-	4.88	6.05	1.17
30x30	-166.03	-166.60	-0.57	100.00	100.57	0.57	-	-	-	5.98	6.96	0.98
10x5	-55.88	-56.19	-0.31	98.77	99.42	0.65	6.42	5.46	-0.96	3.45	4.59	1.05
20x10	-111.04	-111.27	-0.23	100.33	100.64	0.31	-	-	-	4.20	5.32	1.12
30x10	-165.94	-166.43	-0.49	100.89	101.44	0.55	-	-	-	4.34	5.52	1.18
Average			**-0.42**			**0.42**			**-0.73**			**1.02**
Standard deviation			**0.22**			**0.29**			**0.82**			**0.23**

A.3 Output Factors

Table 4 shows the percent output factor differences between measurement and calculation of various square and rectangular fields. The average of output factor difference between measurement and calculation were 0.61±0.85% with the maximum of -1.54% at the largest filed size of 35x35 cm^2.

Table 4 Measured and calculated output factors for various square and rectangular fields.

Field size (cm^2)	Measurement	Calculation	Difference (%)
5x5	0.90	0.89	-0.46
8x8	0.97	0.96	-0.37
12x12	1.03	1.03	-0.13
15x15	1.06	1.06	0.02
20x20	1.10	1.10	0.00
25x25	1.13	1.13	0.02
30x30	1.16	1.14	-1.49
35x35	1.17	1.15	-1.54
10x5	0.94	0.93	-1.22
5x10	0.93	0.94	0.59
5x15	0.95	0.96	1.05
5x20	0.95	0.96	1.12
5x30	0.96	0.97	1.14
10x15	1.02	1.03	0.42
10x20	1.04	1.04	0.57
10x25	1.04	1.05	0.71
10x30	1.05	1.06	0.80
20x10	1.04	1.04	-0.44
30x10	1.06	1.05	-0.85
Average			**0.61**
Standard deviation			**0.85**

B. Clinical applications

B.1 Homogeneous medium in solid water phantom

Figure 5 is the isocenter dose differences between measurement and calculation for 3D-CRT, IMRT and VMAT plans in head (No. 1 to 5), chest (No. 6 to 10) and pelvic (No. 11 to 15) regions, while the data in Table 5, Table 6, and Table 7 show the results performed for the clinical situation in 3D-CRT, IMRT, and VMAT plans, respectively. The dose comparison of head, chest and pelvic regions between calculating from Acuros XB and measuring from ionization chamber in homogeneous solid water phantom were very good agreement between with average dose differences of only -0.12±0.38% (range from -0.52 to 0.71%), -1.59±0.93% (range from -2.95 to -0.18%), and 0.87±1.24% (range from -1.38 to 2.70%) for 3D-CRT, IMRT, and VMAT plans, respectively.

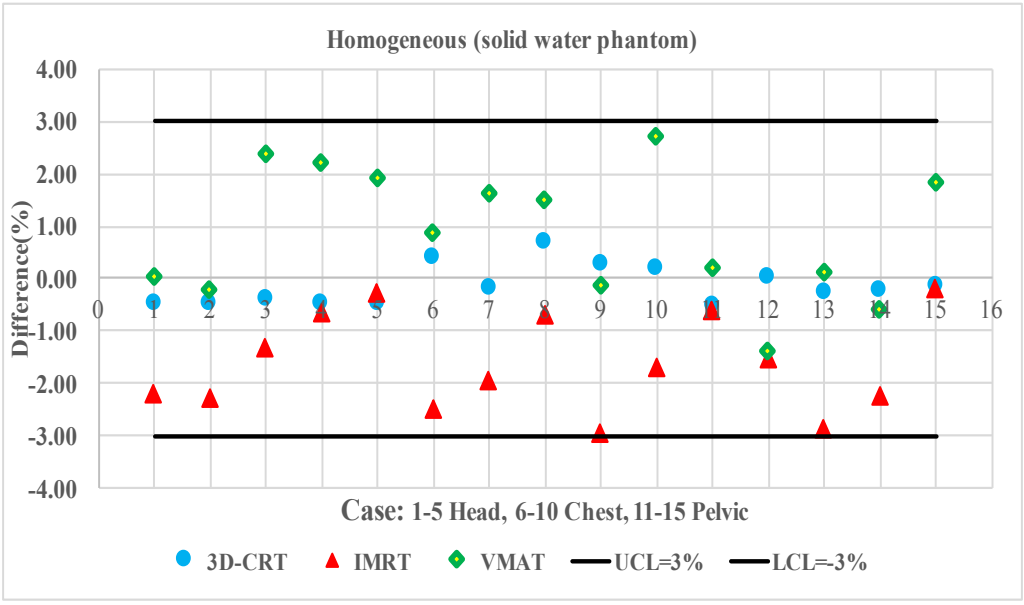

Figure 5 *The percentage of dose difference between measurement and calculation in 3D-CRT, IMRT and VMAT plans of head, chest and pelvic regions in homogeneous solid water phantom.*

Table 5 Dose difference between measurement and calculation in solid water phantom as the homogeneous medium for 3D-CRT technique.

Case No.	Regions	Measurement (cGy)	Calculation (cGy)	Difference (%)
1	Head	301.35	300	-0.45
2	Head	301.35	300	-0.45
3	Head	301.16	300	-0.38
4	Head	301.40	300	-0.47
5	Head	301.35	300	-0.45
6	Chest	298.76	300	0.42
7	Chest	300.52	300	-0.17
8	Chest	198.58	200	0.71
9	Chest	299.10	300	0.30
10	Chest	199.61	200	0.19
11	Pelvic	180.94	180	-0.52
12	Pelvic	179.96	180	0.02
13	Pelvic	180.45	180	-0.25
14	Pelvic	180.35	180	-0.19
15	Pelvic	180.35	180	-0.14
Average				**-0.12**
Standard deviation				**0.38**

Table 6 Dose difference between measurement and calculation in solid water phantom as the homogeneous medium for IMRT technique.

Case No.	Regions	Measurement (cGy)	Calculation (cGy)	Difference (%)
1	Head	306.75	300	-2.20
2	Head	204.69	200	-2.29
3	Head	202.63	200	-1.30
4	Head	201.28	200	-0.63
5	Head	200.53	200	-0.26
6	Chest	205.12	200	-2.49
7	Chest	203.95	200	-1.94
8	Chest	201.36	200	-0.67
9	Chest	206.07	200	-2.95
10	Chest	203.45	200	-1.70
11	Pelvic	181.09	180	-0.60
12	Pelvic	203.08	200	-1.52
13	Pelvic	236.77	230	-2.85
14	Pelvic	229.10	224	-2.22
15	Pelvic	200.37	200	-0.18
Average				**-1.59**
Standard deviation				**0.93**

Table 7 Dose difference between measurement and calculation in solid water phantom as the homogeneous medium for VMAT technique.

Case No.	Regions	Measurement (cGy)	Calculation (cGy)	Difference (%)
1	Head	179.91	180	0.05
2	Head	200.44	200	-0.22
3	Head	175.84	180	2.37
4	Head	215.20	220	2.23
5	Head	176.61	180	1.92
6	Chest	118.94	120	0.89
7	Chest	196.80	200	1.63
8	Chest	197.01	200	1.52
9	Chest	212.40	212.1	-0.14
10	Chest	259.00	266	2.70
11	Pelvic	179.65	180	0.19
12	Pelvic	182.51	180	-1.38
13	Pelvic	199.74	200	0.13
14	Pelvic	181.09	180	-0.60
15	Pelvic	294.62	300	1.82
Average				**0.87**
Standard deviation				**1.24**

B.2 Inhomogeneous medium in CIRS thorax phantom

Table 8, 9, and 10 are the dose differences between measurement and calculation for 3D-CRT, IMRT, and VMAT plans in CIRS thorax phantom, respectively. The average dose difference in 3D-CRT was only 0.27±0.29% with the range from -0.37% to 0.61%. The average dose difference in IMRT was -0.60±1.05% with the range from -2.27% to 0.53%. The VMAT showed the average dose difference of -1.12±0.44% with the range from -1.90% to -0.34%. The data are presented in Figure 6 that showed the dose differences for 3D-CRT, IMRT and VMAT plans in CIRS thorax phantom for head (no. 1 to 5), chest (no. 6 to 10) and pelvic (no. 11 to 15) regions. In 3D-CRT, the differences were almost the same pattern with the results from homogeneous phantom. The 3D-CRT (circle) exhibited lesser deviation of dose differences compared with IMRT (triangle) and VMAT (diamond) techniques.

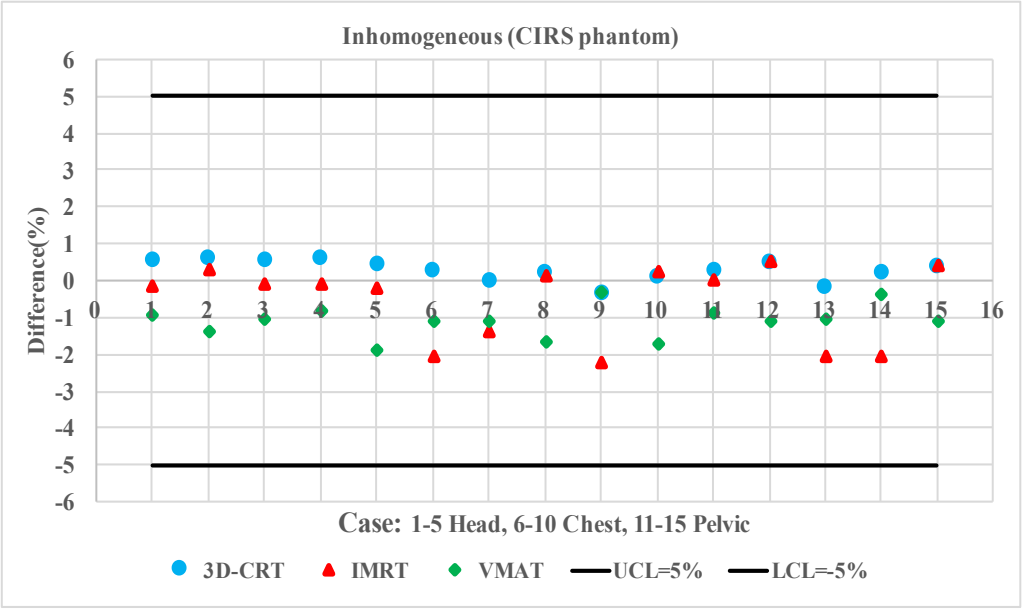

Figure 6 *Percentage of dose difference between measurement and calculation in 3D-CRT, IMRT and VMAT plans of head, chest and pelvic region in CIRS thorax inhomogeneous phantom.*

Table 8 Dose difference between measurement and calculation in CIRS thorax phantom as the inhomogeneous medium for 3D-CRT technique.

Case No.	Regions	Measurement (cGy)	Calculation (cGy)	Difference (%)
1	Head	298.44	300	0.52
2	Head	298.17	300	0.61
3	Head	298.44	300	0.52
4	Head	298.17	300	0.61
5	Head	298.70	300	0.43
6	Chest	299.24	300	0.25
7	Chest	300.04	300	-0.01
8	Chest	199.60	200	0.20
9	Chest	301.10	300	-0.37
10	Chest	199.84	200	0.08
11	Pelvic	179.17	180	0.46
12	Pelvic	180.32	180	-0.18
13	Pelvic	179.65	180	0.20
14	Pelvic	179.31	180	0.38
15	Pelvic	179.25	180	0.27
Average				**0.27**
Standard deviation				**0.29**

Table 9 Dose difference between measurement and calculation in the CIRS thorax phantom as the inhomogeneous medium for IMRT technique.

Case No.	Regions	Measurement (cGy)	Calculation (cGy)	Difference (%)
1	Head	300.51	300	-0.17
2	Head	199.43	200	0.29
3	Head	200.18	200	-0.09
4	Head	200.18	200	-0.09
5	Head	200.45	200	-0.22
6	Chest	202.88	200	-1.42
7	Chest	199.80	200	0.10
8	Chest	204.64	200	-2.27
9	Chest	199.51	200	0.25
10	Chest	202.88	200	-1.42
11	Pelvic	180.04	180	-0.02
12	Pelvic	198.95	200	0.53
13	Pelvic	234.93	230	-2.10
14	Pelvic	228.73	224	-2.07
15	Pelvic	199.22	200	0.39
Average				**-0.60**
Standard deviation				**1.05**

Table 10 Dose difference between measurement and calculation in the CIRS thorax phantom as the inhomogeneous medium for VMAT technique.

Case No.	Regions	Measurement (cGy)	Calculation (cGy)	Difference (%)
1	Head	222.08	220	-0.94
2	Head	182.53	180	-1.39
3	Head	202.19	200	-1.08
4	Head	181.53	180	-0.85
5	Head	203.88	200	-1.90
6	Chest	121.38	120	-1.14
7	Chest	303.45	300	-1.14
8	Chest	203.39	200	-1.67
9	Chest	200.68	200	-0.34
10	Chest	203.56	200	-1.17
11	Pelvic	302.65	300	-0.87
12	Pelvic	182.04	180	-1.12
13	Pelvic	204.71	202.5	-1.08
14	Pelvic	200.79	200	-0.39
15	Pelvic	218.46	216	-1.13
Average				**-1.12**
Standard deviation				**0.44**

Discussion

A. Basic beam characteristics:

A.1 Percentage depth doses

From Figure 3 and Table 1, the very good agreement between calculated and measured PDD for all fields were observed in the linear part of the curve but slightly difference at the build-up region and at very lower dose of deeper depth. The results of average difference of δ_1 and δ_2 in PDD in this study agreed with Hoffmann L et al.[4] studied who showed the differences of PDD within 1% in dose and 1 mm in distance to agreement. Following the IAEA TRS 430, the tolerance limit of δ_1 is 2.0% and δ_2 is 2.0 mm. The maximum dose difference at 10 cm depth, δ_1, was found at -1.16% for 20x20 cm^2 field size, while the maximum distance difference at 90% dose before buildup region, δ_2, was 1.11 mm for 20x20 cm^2 field size. These small errors might be due to the setup uncertainty during measurement and error of dose calculation algorithm in the buildup region.

A.2 Beam profiles

The excellent agreement between measured and calculated beam profiles in both in and cross-planes were found in all field sizes, however, the curves showed slightly differences at the penumbra region and at very low dose. When the quantitative evaluation was used, we found that the differences were within the acceptability criteria for external dose calculation according to IAEA TRS 430 of 2 mm for δ_2, 3% for δ_3, 3% for δ_4, and 2 mm for $\delta_{50\text{-}90}$ as shown in Table 2 and 3 for in-plane and cross-plane results, respectively. The δ_4 in the large field from 20 cm in any side cannot interpret the results due to the limitation of water phantom size for beam scanning.

A.3 Output Factors

From the results of output factors, the average difference between measurement and calculation were 0.61±0.85% and it seems to be the lesser deviation was detected at the smaller field. This study showed slightly larger differences than L. Hoffmann et al.[2], who presented the maximum deviation of output factor at 0.50% that might be due to the small chamber selected in our measurement that difference from 0.6 cc farmer chamber from Hoffmann. However, our output factor results were still within the limitation of 2.00% for all field sizes.[7]

B. Clinical applications

B.1 Homogeneous medium in solid water phantom

The 3D-CRT plans showed almost comparable and small deviation of isocenter dose difference between planning and calculation in all cases as shown in circle symbol in Figure 5 that might be due to the simple plan in 3D-CRT. On the other hand, the average dose differences of IMRT and VMAT plans were higher than in 3D-CRT technique because IMRT and VMAT were the complicated plans and the chamber position may be located in the high dose gradient region. However, the errors from all of the test cases were still within ±3.00% limitation recommended by IAEA TRS430.[3] The results were agreed with Han T et al.[8] studied who presented the dose differences in the range of 0.10% to 3.60%. The variation among head, chest and

pelvic regions were not much different because these plans were recalculated in homogeneous water phantom. Therefore, the inhomogeneity correction was not considered.

B.2 Inhomogeneous medium in CIRS thorax phantom

The CIRS thorax phantom was selected as the inhomogeneous medium and used to compare the dose differences at isocenter between measurement and calculation. The results showed very good agreement in all treatment regions and techniques as shown in Figure 6 and Table 8 to 10 because Acuros XB algorithm was designed to improve the accuracy dose calculation in heterogeneity medium than the previous calculation algorithm, AAA. The variation of dose difference among regions was not much in 3D-CRT but slightly fluctuated in IMRT and VMAT due to the plan complexity of advanced treatment techniques that very sensitive to position of chamber. Among the regions, IMRT and VMAT plans displayed less variation in head compared to chest and pelvic due to lesser inhomogeneity area in head area.

Conclusion

PDDs and profiles between measurement and calculation are in good agreement except the tails of beam profiles for very small dose and small gradient. The average output differences were 0.61±0.85%. The clinical cases are very excellent agreement between measurement and calculation in both homogeneous (within 3.00%) and inhomogeneous (within 5.00%) phantoms for all 3D, IMRT and VMAT techniques. Therefore, the Acuros XB algorithm is acceptable for dose calculation in external beam radiotherapy in case of isocenter point dose verification. However, to fulfill the verification of dose calculation algorithm in clinical situation, the dose distribution in comparison with gamma criteria analysis should be further study in IMRT and VMAT planning.

Conflicts of interest

Conflicts of interest

References

[1] Lloyd SA, Ansbacher W. Evaluation of an analytic linear Boltzmann transport equation solver for high-density inhomogeneities. Med Phys 2013; 40:0117071-5.

[2] Gregory AF, Wareing T, Archambault Y, Thompson S. Acuros XB advanced dose calculation for the Eclipse™ treatment planning system. Varian Medical System, Palo, Alto, CA. 2015. Avaliable from: https://www.varian.com/sites/default/files/resource_attachments/AcurosXBClinicalPerspectives_0.pdf

[3] Vassiliev ON, Wareing TA, McGhee J, Failla G, Salehpour MR, Mourtada F. Validation of a new grid-based Boltzmann equation for solver dose calculation in radiotherapy with photon beams. Phys Med Biol 2010; 55: 581-98.

[4] Hoffmann L, Jørgensen MB, Muren LP, Petersen JB., Clinical validation of the Acuros XB photon dose calculation algorithm, a grid-based Boltzmann equation solver. Acta Oncol 2012; 51(3): 376-85.

[5] Zifodya JM, Challens CH, Hsieh WL, From AAA to Acuros XB-clinical implications of selecting either Acuros XB dose-to-water or dose-to-medium. Australas Phys Eng Sci Med 2016; 39(2): 431-9.

[6] Yeh PCY, Lee CC, Chao TC, Tung CJ. Monte Carlo evaluation of Acuros XB dose calculation Algorithm for intensity modulated radiation therapy of nasopharyngeal carcinoma. Rad Phys Chem 2017;140: 419-22.

[7] International Atomic Energy Agency. Commissioning and quality assurance of computerized planning systems for radiation treatment of cancer: TRS Report No 430. Vienna; Austria: 2004.

[8] Han T, Mourtada F, Kisling K, Mikell J, Followill D, Howell R. Experimental validation of deterministic Acuros XB algorithm for IMRT and VMAT dose calculations with the Radiological Physics Center's head and neck phantom. Med Phys 2012; 39(4): 2193-202.